# Vacuum Contact Drying of Free Flowing Mechanically Agitated Multigranular Packings

## Vakuum-Kontakttrocknung von rieselfähigen, mechanisch durchmischten, polydispersen Schüttungen

E. TSOTSAS and E. U. SCHLÜNDER

*Institut für Thermische Verfahrenstechnik, Universität Karlsruhe (TH), Postfach 6980, 7500 Karlsruhe 1 (F.R.G.)*

(Received May 6, 1986)

## Abstract

The influence of diameter dispersity on the drying rate curve during vacuum contact drying of multigranular packings is discussed. Experimental investigations have been carried out in a disc dryer using free flowing bi- and polydispersed packings of porous granular material. The theoretical evaluation is based on an extended version of the penetration model introduced by Mollekopf and Schlünder for packings of equal particles. De-mixing occurring during mechanical agitation seems to be of great importance for the drying process. In order to calculate drying rates the de-mixing patterns must be known. These patterns can differ depending on the geometry of the apparatus.

## Kurzfassung

Der Einfluss der Dispersität des Schüttgutes auf die Trocknungsverlaufskurve bei der Vakuum-Trocknung in Kontaktapparaten wurde experimentell und theoretisch untersucht. Rieselfähige bi- und polydisperse Schüttungen aus kapillarporösen, keramischen Partikeln wurden in einem Tellertrockner getrocknet. Zur Beschreibung der Versuchsergebnisse ist das von Mollekopf und Schlünder für monodisperse Schüttungen eingeführte Penetrationsmodell erweitert worden. Es stellte sich heraus, dass bei der Kontakttrocknung polydisperser Schüttungen eventuell auftretende Entmischungserscheinungen die Trocknungsverlaufskurve stark beeinflussen. Das gleiche gilt für Schüttungen, deren Partikeln sich in Dichte, Form oder Beschaffenheit unterscheiden. Um solche Einflüsse rechnerisch zu erfassen, müssen die von der Bauart des Trockners abhängigen Entmischungsmuster bekannt sein.

## Synopse

*Die Vakuum-Kontakttrocknung wird gewöhnlich in Teller- oder Trommelapparaten durchgeführt, wobei die Schüttung mechanisch durchmischt wird. Zur Auslegung solcher Kontaktapparate benötigt man Trocknungsverlaufskurven. Eine Methode zur Vorausberechnung dieser Trocknungsverlaufskurven wurde in dieser Zeitschrift ausführlich präsentiert (Schlünder und Mollekopf, ref. 5). Diese Autoren nehmen an, dass von den Wärmeübergangs- und Stofftransportwiderständen, die bei der Vakuum-Kontakttrocknung von Bedeutung sein können (Bild 1), nur der Kontaktwiderstand zwischen Heizfläche und Schüttung $1/\alpha_{ws}$ sowie auch der Wärmeeindringwiderstand der Schüttung $1/\alpha_{sb}$ massgeblich sind. Der Wärmeeindringwiderstand der Schüttung ist eine Funktion der Intensität der Durchmischung, die mit einer Mischgüte-Kennzahl $N_{mix}$ beschrieben wird (Gl. (1)). $N_{mix}$ ist eine rein mechanische Eigenschaft des Systems und wurde für verschiedene Trocknerbauarten anhand von Messungen ermittelt. Zur Berechnung von $\alpha_{sb}$ wird die Neumannsche Lösung der Fourierschen Wärmeleitungsgleichung herangezogen. Ziel dieser Arbeit ist es, dieses Modell, auch Penetrationsmodell genannt (Bild 2), für bi- und polydisperse Kugelschüttungen zu erweitern. Für solche Fälle, bei denen das zu trocknende Granulat eine merkliche Durchmesserdispersität aufweist, sind weder experimentelle Untersuchungen noch theoretische Berechnungsansätze bekannt.*

*Bei polydispersen Schüttungen wird grundsätzlich zwischen stochastisch homogenen und unterstochastischen Schüttungen unterschieden. Bei einer stochastisch homogenen Schüttung ist die lokale Zusammensetzung überall die gleiche, bei einer unterstochastischen ist diese Bedingung nicht gewährleistet, d.h. es treten Entmischungserscheinungen auf.*

*Das Zumischen feinen Granulats in eine grobe Schüttung sollte eine erhebliche Verbesserung der Trocknungsgeschwindigkeit bewirken, falls der Zustand stochastischer Homogenität vorliegt (Bild 5). Die*

*Trocknungsverlaufskurven in Bild 5 sind mit dem unveränderten Penetrationsmodell berechnet worden. Es wurden geeignete Ansätze verwendet, um den Einfluss der Schüttungszusammensetzung auf die Wärmeleitfähigkeit [10], auf die Schüttungsporosität bzw. -dichte, [11, 12] und Bild 3, sowie auch auf den Wärmeübergangswiderstand Wand-Schüttung, Bild 4, zu berücksichtigen.*

*Es stellt sich die Frage, ob unter praktischen Trocknungsbedingungen eine polydisperse Schüttung als homogen angesehen werden darf. Um diese Frage zu beantworten, wurden experimentelle Untersuchungen durchgeführt. Es wurde ein absatzweise betriebener Tellertrockner mit einem Heizplattendurchmesser von 240 mm verwendet. Als Rührorgan diente ein zweiarmiger Besenrührer (Bild 7). Die Versuchsanlage ist im Bild 6 schematisch abgebildet. Beim Versuchsmaterial handelte es sich, wie auch bei früheren Untersuchungen [15, 4, 1], um kapillarporöse, kugelförmige Aluminiumsilikatpartikeln im Durchmesserbereich von 0,4 bis 5,0 mm. Dieses Material ist kaum hygroskopisch und wurde immer in rieselfähigem Zustand in die Anlage eingespeist. Es wurden bidisperse und polydisperse Schüttungen bei konstanter Heizplattentemperatur, Kammerdruck und Rührerdrehzahl getrocknet und die Trocknungsverlaufskurven aufgenommen.*

*Typische gemessene Trocknungsverlaufskurven für bidisperse Schüttungen sind in den Bildern 11 und 13 zu sehen. Die Verläufe sind grundsätzlich verschieden von den im Bild 5 dargestellten berechneten Kurven. Der Grund dafür sind stark ausgeprägte Entmischungserscheinungen, die im Tellertrockner auftreten. Die Entmischung hat den Charakter einer weitgehenden Schichtung, wobei das feine Granulat die Heizfläche belegt und das grobe darüber liegt. Dieses Verhalten konnte auch optisch sehr gut beobachtet werden (Bild 12). Polydisperse Schüttungen weisen einen ähnlichen Trocknungsverlauf wie die bidispersen auf (Bild 14).*

*Von der Annahme ausgehend, dass die Entmischung den Charakter einer vollkommenen Schichtung der zwei Einzelfraktionen hat, kann man den gesamten Trockungsvorgang in zwei Bereiche unterteilen. Im ersten Bereich trocknet die feine Schicht aus; das ursprüngliche Modell ist unmittelbar anwendbar. Im zweiten Bereich muss die Wärme durch die schon trockene, durchmischte Schicht aus feinen Partikeln an die in der groben Schüttung wandernde Trocknungsfront übertragen werden (s. Bild 16). Eine leicht abgeänderte Form der Neumannschen Lösung kann angewendet werden, und der Trocknungsvorgang ist im Rahmen des Penetrationsmodells berechenbar. Zur Wiedergabe der Versuchsergebnisse (durchgezogene Linien in den Bildern 17(a)–(c) (s. auch Lit. 14)), wurde der Wärmeeindringkoeffizient der feinen Schicht* $\alpha_{sb,f}^{dry}$ *(Gl. (6a)) mit einem Korrekturfaktor versehen (Gl. (16b)). Dieser soll der Abweichung der Realität vom angenommenen Zustand der idealen Schichtung Rechnung tragen und hatte für alle Versuche den Wert 2. Die zur Erfassung des Einflusses der mechanischen Durchmischung notwendigen* $N_{mix}$*-Werte für die grobe und die feine Schicht (Gln. (16a) und (16b)) wurden von Versuchen mit den entsprechenden monodispersen Schüttungen übernommen (Bilder 8, 9 und 10 sowie auch Tabelle 1). Diese Werte sind ausserdem von experimentellen Daten bei der Wärmeübertragung an trockene durchmischte Schüttungen [8, 15], sowie auch bei der Kontakttrocknung in Inertgas-Atmosphäre [9] für den eingesetzten Trockner und das Rührorgan belegt.*

*Im letzten Abschnitt werden die aus der Literatur bekannten [16], in einem Trommeltrockner auftretenden Entmischungsmuster diskutiert und mögliche Wege der Vorausberechnung der Trocknungsverlaufskurve unterstochastischer Schüttungen in solchen Apparaten kurz angesprochen.*

## 1. Introduction

In contact drying the heat needed to vaporize the water or other liquid is transferred to the particulate material through a wall. Contact drying is commonly carried out in disc dryers and in drum dryers. In order to achieve uniform drying the particle layers are agitated mechanically. The agitating elements in a disc dryer are stirrers, scrapers or paddles. There are rotating drum dryers with or without additional stirring elements as well as static drum dryers with flyers inside. Contact dryers can be run without an inert gas atmosphere (vacuum contact drying). This may be advantageous in many cases or imperative.

For the design of all kinds of contact dryers the 'drying rate curve', which correlates the drying rate $\dot{m}$ (in kg vapour per m$^2$ hot surface area per hour) with the average moisture content $X$ of the product (in kg liquid per kg dry material) is needed. The drying rate is apparently affected by both the heat supply and the vapour removal. In general, the heat supplied must overcome three heat transfer resistances: the contact resistance at the hot surface, the penetration resistance of the bulk, and the penetration resistance of the particle. On the other hand, the vapour to be removed must overcome two mass transfer resistances: the permeation resistance of the porous particle and the permeation resistance of the bulk. In the absence of inert gas, the mass transfer resistances are flow resistances. For a non-agitated packed bed all the above-mentioned resistances lie in series (Fig. 1). However, if the particulate material is mechanically agitated, we expect a random distribution of dry, partly wet and wet material, thus forming a random distribution of transport resistances partly in series and partly in parallel.

In order to describe the rather complicated situation by a suitable model, all authors take into consideration some of the resistances which are assumed to be rate controlling. The classical approach is that of the single sphere. A sharp drying front is supposed to move into a spherical particle which is considered as representative for the whole bed. The heat and mass transfer resistances in this particle are supposed to be rate controlling. An additional heat transfer resistance from the heating surface to the particle can sometimes be identified as a contact resistance. Other authors try to introduce in this resistance penetration terms which must be empirically correlated [1–3].

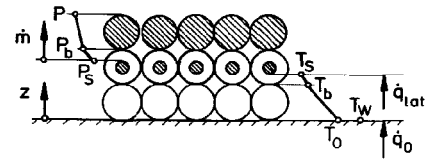


**Heat in**

Contact : $\frac{1}{\alpha_{WS}} = \frac{T_W - T_0}{\dot{q}_0}$

Bulk penetration : $\frac{1}{\alpha_{sb}} = \frac{T_0 - T_b}{\dot{q}_0}$

Particle penetrat.: $\frac{1}{\alpha_P} = \frac{T_b - T_S}{\dot{q}_{lat}}$

**Mass out**

Particle permeation: $\frac{1}{\beta_P} = \frac{P_S - P_b}{\dot{m}}$

Bulk permeation : $\frac{1}{\beta_b} = \frac{P_b - P}{\dot{m}}$

Fig. 1. Heat and mass transfer resistances in contact drying.

The model of the single sphere may be appropriate for very coarse particles and very high inner resistances. In all other cases another approach introduced by Mollekopf and Schlünder [4, 5] seems to describe the process better. This model, sometimes called the penetration model, will be the basis of this paper and is therefore briefly outlined in the next section. Thereafter this model, which was initially derived for monodispersed material, is extended to multigranular packings. The restrictions of the material being free flowing and not hygroscopic remain.

## 2. The model for monodispersed packings

Mollekopf and Schlünder [4, 5] regard vacuum contact drying of free flowing mechanically agitated particulate material as a purely heat transfer controlled process. They consider the contact resistance at the hot surface and the penetration resistance of the bulk to be rate controlling.

The contact heat transfer coefficient $\alpha_{ws}$ can be predicted from first principles [5, 6] and is a strong function of the particle diameter. Its value remains constant with good accuracy during a drying process at constant pressure and heating plate temperature and sets an upper limit for the drying rate.

Unlike $1/\alpha_{ws}$, which is completely independent of mechanical agitation, the bulk penetration resistance $1/\alpha_{sb}$ is a function of mixing intensity. Hence, in order to evaluate $\alpha_{sb}$ a model adequately describing the effect of random particle motion is needed. For this purpose Mollekopf and Schlünder use the so-called penetration theory. The steady mixing process is replaced by a sequence of unsteady mixing steps. During a certain (fictitious) period of length $t_R$ the bulk is static. A distinct drying front penetrates from the hot surface into the bulk. Between the moving front and the hot surface all particles are dry; beyond the front all particles are wet. When the static period ends at $t = t_R$ the bulk is perfectly mixed. Thereafter, the drying front moves again into the bulk. This time, however, there are some particles which have already been dried during the first period. This situation is illustrated in Fig. 2. Assuming that the packed bed may be considered as a quasi-continuum obeying Fourier's law of heat transfer, one can make use of Neumann's solution to calculate the location of the drying front, the transient temperature profiles, the bulk penetration resistance and finally the drying rate during each static period. The overall heat conductivity of the dry packed bed, $\lambda_{bed}$, needed for the calculation can be predicted from standard equations [5, 7].

The remaining problem is to estimate the length of the fictitious static period. This length $t_R$ is postulated to be a function of the time scale of the mixing device (reciprocal stirrer speed in $min^{-1}$, drum revolutions per unit time, etc.) and has been defined as

$$t_R = t_{mix} N_{mix} \tag{1}$$

The quantity $N_{mix}$, the so-called 'mixing number', is a mechanical property of the mixing device connected with the mechanical properties of the product, and a function of the time scale of the stirrer. It must be fitted to experimental results. $N_{mix}$ simply says how often the mixing device must have turned around before the product has been ideally mixed once (within the scope of the penetration model).

The model briefly outlined above yielded very good agreement between experiment and calculation for numerous drying rate curves measured in various contact dryers. The pressure was varied between 1 and 200 mbar, the overall temperature difference between

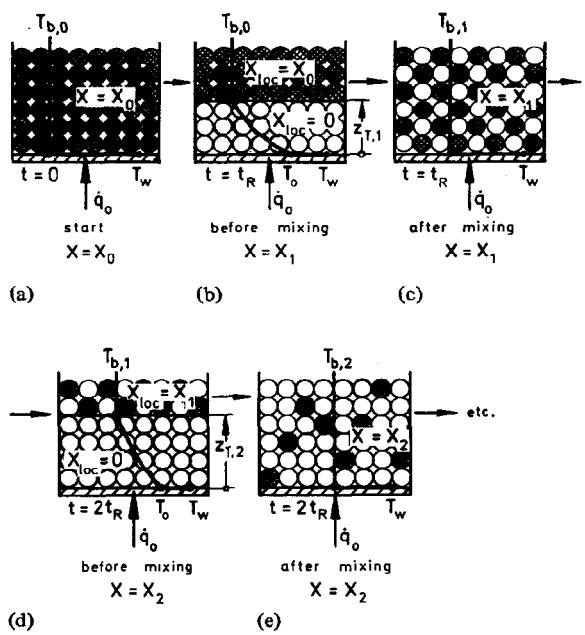


Fig. 2. Illustration of the contact drying model for monodispersed material.

10 and 200 °C, the particle diameter between 170 and 6600 $\mu$m and the speed of the stirrer between 0.2 and 130 rev $min^{-1}$. The granulate material dried was magnesium silicate, aluminium silicate, Perlkontakt and PVC. The mixing number was found to lie between 2 and 25 and has been correlated for each dryer type to the Froude number. The same values of $N_{mix}$ can be used to describe the heat transfer from the surface of immersed bodies to stirred beds of *dry* particulate material [8], as well as for contact drying in an inert gas atmosphere [9].

## 3. Contact drying of multigranular packings

In order to apply Neumann's solution to calculate the drying rate, the properties of the dry bed, such as the density $\rho_{bed}$, the specific heat capacity $c_{bed}$ and the effective thermal conductivity $\lambda_{bed}$, must be constant (independent of temperature and independent of the length coordinate perpendicular to the heating surface). The same must be valid for the product $X\,\Delta h_{ev}$, which describes the intensity of the latent heat sink in the wet bed. In the following we shall discuss whether these assumptions are fulfilled in the case of multigranular packings. We distinguish between stochastic homogeneous and understochastic (inhomogeneous) packings.

### *3.1. Stochastic homogeneous multigranular packings*

A multigranular packing is said to be stochastic homogeneous if the probability of a particle lying at a specific location in the bed is the same for all possible locations. From this definition it follows that all physical properties of such a packing are independent of the length coordinate. Neumann's solution can thus be used to predict the bulk penetration coefficient and the drying rate. One should, however, dispose of adequate equations for the calculation of the dispersity dependent properties of the packing. Such properties are the effective thermal conductivity $\lambda_{bed}$, the density $\rho_{bed}$ or the corresponding bed porosity $\psi$, and the wall-to-first-particle-layer heat transfer coefficient $\alpha_{ws}$.

#### *3.1.1. Prediction of $\lambda_{bed}$, $\psi$ and $\alpha_{ws}$ for homogeneous multigranular packings*

To predict the heat conductivity of the dry bulk material, the method introduced by Bauer and Schlünder was used. In ref. 10 calculated values of the overall heat conductivity of binary mixtures of spheres are compared with measured values. For a constant volumetric composition of the mixture the number of contact points between spheres and consequently the heat conductivity of the bed increases with increasing diameter ratio of the fractions involved. For a constant diameter ratio the number of contact points changes with the composition of the mixture, so that in each case a maximal value is attained.

A model first proposed by Wise [11] (see also ref. 12) was used for the calculation of the bed porosity. Assuming that all spheres touch their neighbours the structure of a random packing of spheres of different size can be reduced to a system composed of known tetrahedral sub-units. The frequency distribution of these sub-units can be calculated from the sphere size distribution using simple statistics and geometry. The overall porosity is then given by the sum of the porosities of the individual tetrahedra weighted by their relative frequencies. The absolute values obtained are unrealistically low, but can be corrected using a multiplying factor to simulate a moving apart of all the spheres. When corrected in this manner, the model yields at least a qualitatively correct description of the relatively well-known variation of the porosity with composition for binary mixtures of spheres. The porosity of the packing is maximal for equal spheres ($\psi = 0.40$), diminishing with any distribution in particle size.

Plotting the porosity of a binary mixture over the mixture proportion yields non-symmetric V-curves. The addition of a few small spheres to a packing of large ones produces a large change in porosity. This change is all the more marked the greater the diameter ratio. The model briefly outlined tends to underestimate the porosity of beds containing a small amount of fines (see Fig. 3), although it has been regarded as advantageous in comparison to other more exact approaches (see ref. 13), because no fitting on experimental data is needed. The calculation for polydispersed packings becomes cumbersome. In order to save calculational effort such packings have been simulated by bidispersed ones (see also ref. 14).

A very similar method has been used to predict the heat transfer coefficient $\alpha_{ws}$ of bidispersed stochastic homogeneous packings. The elementary unit of the structure in this case is an orthogonal triangular prism. The contact heat transfer coefficient calculated in this

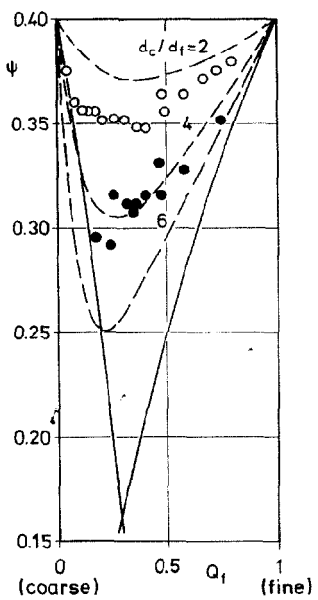


Fig. 3. Porosity of binary mixture of particles. Calculated porosities (from ref. 12, Fig. 5) compared with measured data from ref. 13. ○, $d_c/d_f \cong 2$; ●, $d_c/d_f \cong 4$; ——, limiting curves according to ref. 13; — — —, calculated according to ref. 12.

way is a monotonically increasing convex function of the proportion of fine-grained product in the mixture (Fig. 4). Although experimental values of $\alpha_{ws}$ for such cases fail, the calculated curves appear to be reasonable.

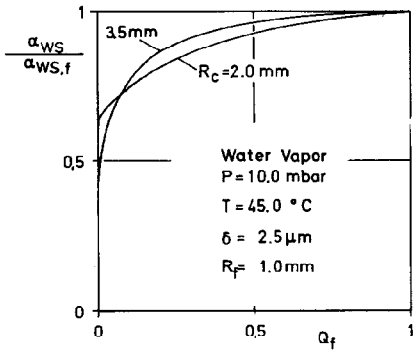


Fig. 4. Calculated wall-to-bed heat transfer coefficients for stochastic homogeneous packings of unequal spheres. $Q_f$ is the amount of fines in the packing. $\alpha_{ws,f}$ is the heat transfer coefficient to the monodispersed bed of fine granulate.

*3.1.2. Calculated drying rate curves for stochastic homogeneous multigranular packings*

Figure 5 shows calculated drying rate curves for a bidispersed stochastic homogeneous packing. $Q_f$ is the mass proportion of fines in the packed bed. For $Q_f = 0$ we have the drying rate curve of the coarse granulate. Adding fine product causes a rapid increase of drying rate (see curve for $Q_f = 0.05$). This can be explained with the increased density, thermal conductivity and contact coefficient of the bidispersed packing in comparison to the coarse monodispersed one. A maximal drying rate is attained for a $Q_f$ of about 0.45. Further addition of small particles to the mixture results in a decrease of the drying rate. This effect is due to the effective bed conductivity and the bed density decreasing after having reached a maximum. For $Q_f = 1$ we obtain the drying rate curve of the fine product.

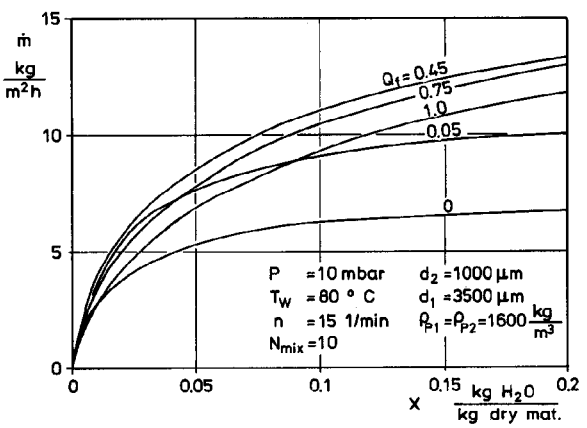


Fig. 5. Calculated drying rate curves for several stochastic homogeneous bidispersed packings.

The behaviour illustrated in Fig. 5 could be of great practical interest, for mixing of small particles in a bed of coarse material would drastically diminish the time or heating area required to accomplish the drying duty. It must, however, be borne in mind that this is the case only if the stirring device can provide and maintain a random distribution of particles in the bed. In the following sections, whether or not this is likely to happen in conventional technical apparatus will be discussed.

*3.2. Understochastic multigranular packings*

When the particles composing a mixture differ in size and/or density, mixing is accompanied by de-mixing. Continued operation of the mixer leads to an equilibrium state in which the components are in most cases partially separated. We shall call such packings understochastic.

A multicomponent packing in a contact dryer is very likely to be understochastic. This would have the following consequences:

(1) The physical properties of the packed bed, such as density and thermal conductivity, would be functions of the distance from the heating plate.

(2) The mixing at the end of the contact time assumed by the penetration model would no longer be able to level the moisture profile. The moisture content, and consequently the intensity of the heat sink, would thus be a function of the distance from the heating plate.

Under such circumstances Neumann's solution cannot be applied to calculate the drying rate. In order to develop a model predicting the drying rate curve, information about the exact character of de-mixing is necessary. This will obviously depend on the type of dryer used. The following sections contain a detailed experimental and theoretical investigation of a disc dryer and a brief discussion about drum dryers.

*3.2.1. Experimental set-up*

The experimental investigations reported have been made with the apparatus shown in Fig. 6 (also see refs. 1, 4 and 14). The drying is carried out in a tubular container (2). The bottom of this container consists of an aluminium plate with a thickness of 5 mm and a diameter of 240 mm, which can be heated by an electrical resistor (4). In order to avoid heat losses a second heating plate is situated below the first one and is kept at the same temperature. For this reason also, the side walls of the container are insulated. The container is placed on a pneumatic device and can be moved down onto a balance (3). In this manner the drying rate can be calculated from the mass change of the entire packing. This procedure excludes mistakes connected with collecting samples and is thus especially advantageous for the multigranular packings used in this investigation. Container and balance lie in an autoclave (1), in order to maintain an atmosphere without inert gas. The granulated product can be mechanically agitated by a stirrer (6) driven by an electric motor (5) through a vacuum-tight coupling (7). The periphery mainly consists of two vacuum pumps (15, 16) and two methanol-cooled condensors (17), to remove the vapour

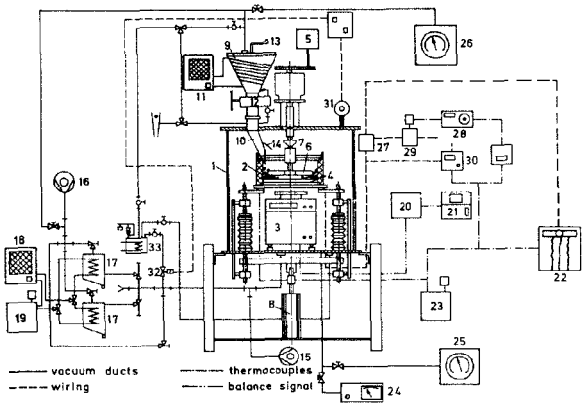


Fig. 6. Experimental set-up (disc dryer).

during the drying process. The methanol is pumped from a storage vessel (19) through two cryostats (18) to the condensors. The temperature of the heating plate and the pressure in the autoclave can be held constant for the duration of a run.

The stirrer shown in Fig. 7, equipped with bristles directly contacting the heating surface, was used as the agitating unit. This provided a good mixing intensity and minimized the grinding of particles between stirrer blade and heating plate.

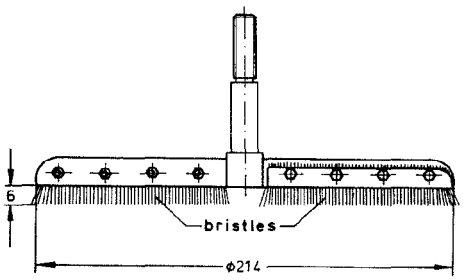


Fig. 7. Stirring equipment (bristle stirrer); dimensions in mm.

*3.2.2. Material*

The granulated material used for the experiments was porous aluminium silicate with a diameter range of 0.4 to 5.0 mm. Narrow fractions of this material gained by sieving were regarded as monodispersed and used to produce bi- and polydispersed packings. The density of dry monodispersed beds, slightly varying with the particle diameter, was about 1000 kg $m^{-3}$ and the specific heat capacity about 800 J $kg^{-1}$ $K^{-1}$. The particle porosity, being a weak function of particle diameter, was about 0.33, the thermal conductivity of the particles was estimated as 1.0 W $m^{-1}$ $K^{-1}$ and the particle roughness as 2.5 $\mu$m. The mean pore diameter, measured by means of mercury porosimetry, was found to be about 0.6 $\mu$m. In order to guarantee the flowability of the heap, the surface moisture of the particles was removed before each run.

*3.2.3. Measured and calculated drying rate curves of monodispersed packings*

In Figs. 8–10 some measured drying rate curves of monodispersed packings are compared with calculated ones. The parameter in the runs shown in Fig. 8 is the particle diameter. The drying rate for fine material is, as expected, much higher than that for coarse material. This results from the contact heat transfer coefficient strongly increasing with decreasing particle size. Figure 9 shows the effect of heating temperature on the drying rate curve. The runs depicted in Fig. 10 demonstrate how intensification of product mixing affects the drying rate. The effect of mixing on the drying rate is low when the actual drying rate comes close to the maximal one. This is the case for coarse-grained material. For such material the contact resistance is rate controlling. The drying rate of fine product is, on the contrary, rather sensitive to variation of the mixing intensity. The bulk resistance of a fine-grained packing tends to become drying rate controlling (for more details see ref. 5). The values of $N_{mix}$ used for the calculation are presented in Table 1.

The values for $n = 15$ $min^{-1}$ were fitted to experimental data. In order to determine $N_{mix}$ for other stirrer

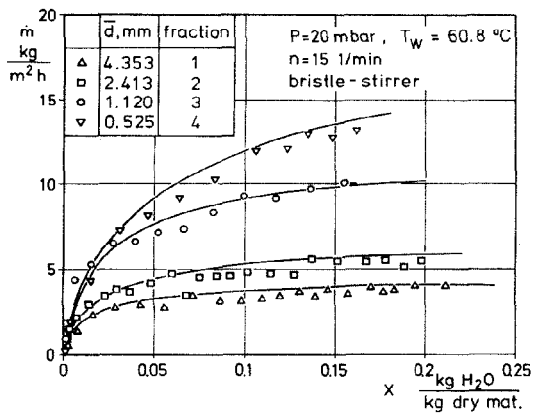


Fig. 8. Influence of particle diameter on the drying rate curve of monodispersed packings.

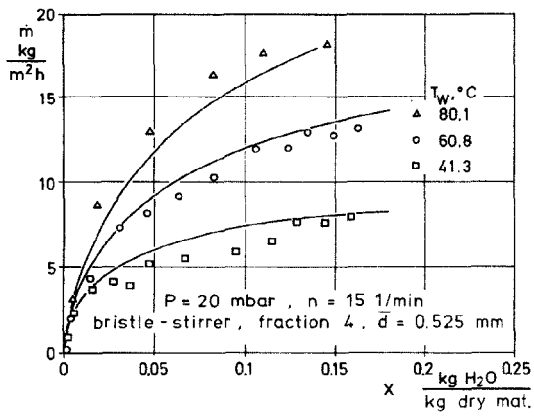


Fig. 9. Influence of hot surface temperature on the drying rate curve of monodispersed packings.

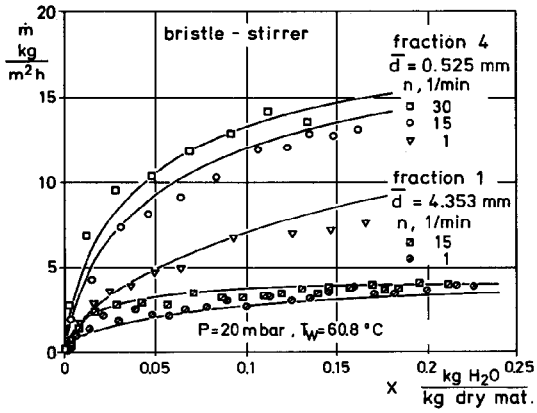


Fig. 10. Influence of the number $n$ of revolutions of the stirrer on the drying rate curve of monodispersed packings.

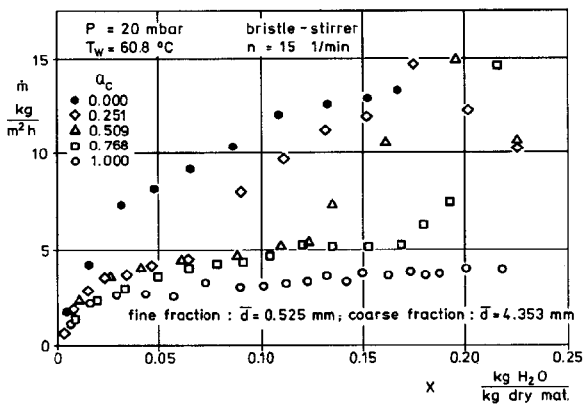


Fig. 11. Measured drying rate curves of bidispersed packings: variation of the composition of the packing.

TABLE 1. Values of $N_{mix}$ used to calculate drying rate curves of monodispersed material

| $n$ (min$^{-1}$) | $d$ ($\mu$m) | | | |
|---|---|---|---|---|
| | 4353 | 2413 | 1120 | 525 |
| 30 | 19.8 | – | 4.0 | 4.0 |
| 15 | 15.0 | 10.0 | 3.0 | 3.0 |
| 1 | 5.1 | – | – | 1.0 |

velocities the correlation given by Mollekopf [4] for disc dryers was used. The mixing quality obviously depends on the particle diameter. This dependency is *not* due to flow or heat penetration resistances in the interior of particles. It is, on the contrary, a mechanical property of the stirring device used here, and was not observed for other forms of agitators. The value of $N_{mix}$ for fine-grained material is almost the same as that used by Schlünder [8] in order to correlate heat transfer measurements made by Wunschmann [15] in an identical disc apparatus equipped with a bistle stirrer.

### *3.2.4. Drying rate curves of bi- and polydispersed packings*

The upper curve depicted in Fig. 11 is the drying rate curve of a fine-grained monodispersed packing ($d$ = 0.525 mm) and the lower the drying rate curve of a coarse-grained one ($d$ = 4.353 mm). The remaining three curves are drying rate curves of bidispersed packings produced by mixing of the fine and the coarse monodispersed granulates in various mass proportions. The drying conditions were the same for all runs in Fig. 11. These results are typical for the form of drying rate curves of bidispersed material in the disc dryer. The drying rate, being at the beginning of drying almost equal to that of fine-grained monodispersed product, decreases more or less steeply with decreasing moisture content of the bed. A bend-point can be observed in all three curves. The location of this point is obviously directly proportional to the proportion of fine product in the bed. The drying rate after the bend-point keeps on decreasing, at first slowly and then for small moisture contents more steeply, approaching null at the end of drying.

The form of the measured drying rate curves is obviously radically different from that expected for stochastic homogeneous packings. The mechanical agitation of multigranular packings in a *disc dryer* is evidently accompanied by *de-mixing* leading to a strongly understochastic packing. Visual observation of the packed bed revealed a far-going segregation of the two monodispersed fractions. The fine particles formed a layer lying on the heating plate and blocking it to coarse material (Fig. 12). This observation can be used to explain the form of the drying rate curves, being divided into two rather distinct regions. In the first region the drying rate is dictated by the drying of fine product in contact with the heating plate, in the second by the drying of coarse particles, the fine ones having already been dried out.

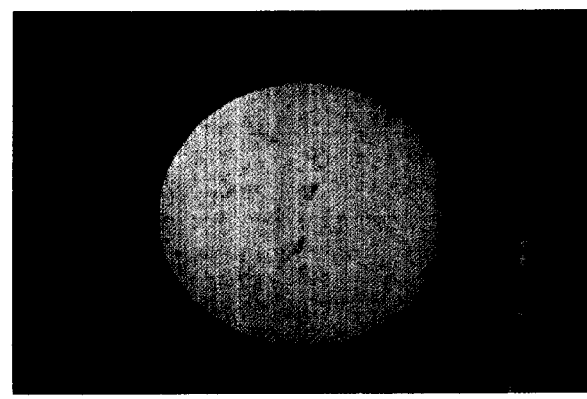

Fig. 12. De-mixing of a binary mixture of spherical particles in a disc apparatus photographed through the bottom of the container ($D$ = 240 mm). The packing was stirred by a bristle stirrer (Fig. 7) with a velocity of 15.0 rev min$^{-1}$. It contained fine particles ($d$ = 0.525, white) and coarse ones ($d$ = 2.413, painted dark). Mass proportion of fines 0.50. The bottom of the container (heating plate of a disc dryer) is almost exclusively covered by fine granulate.

The assumption of drying taking place in two far-reaching distinct regions is supported by the data shown in Fig. 13. For the runs depicted with the triangles *dry* fine product was mixed with wet coarse material. The resulting drying rate curves are identical to the drying rate curve of the fully wetted packing after a moisture content of about 0.12. From the practical point of view the question arises whether mixing of fine product to a coarse packing would increase the drying rate of the latter or not. The presence of fine granulate would in all cases considerably diminish the contact resistance between wall and packing, but would also give rise to an additional heat transfer resistance (heat penetration through the fine layer) not existing for the monodispersed coarse material. The sum of these two resistances is to be compared with the contact resistance of the coarse material, and can, in principle, be lower or higher than this. For the system examined in this work the fine granulate generally caused a slight improvement in the drying rate of the coarse one (see Fig. 11 and ref. 14).

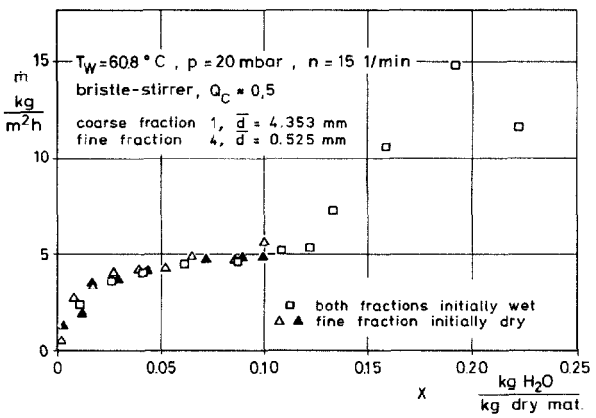


Fig. 13. Illustration of the initial moisture content of fine-grained product having no influence on the drying rate of coarse material, during contact drying of bidispersed packings in a disc dryer.

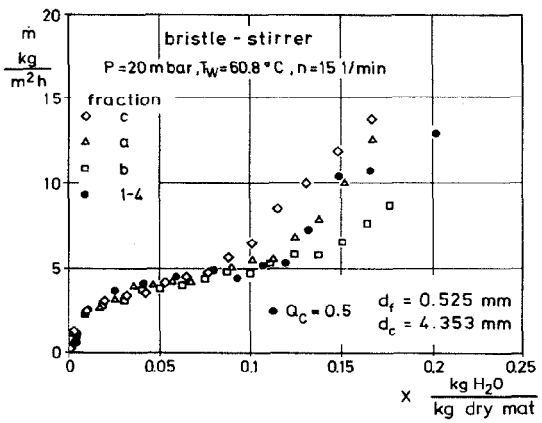


Fig. 14. Measured drying rate curves of polydispersed particulate material in a disc dryer.

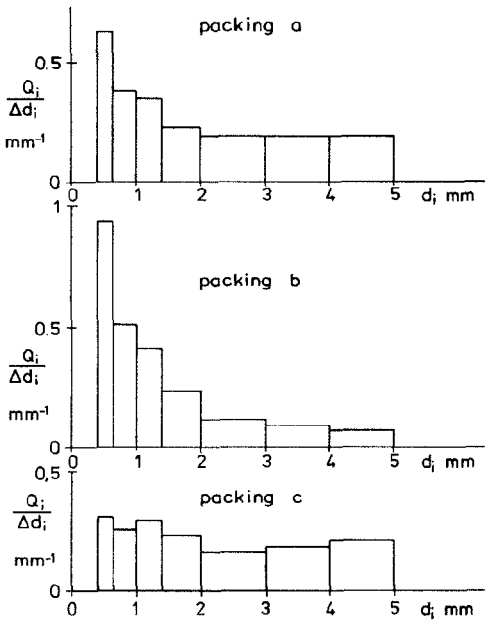


Fig. 15. Composition of the polydispersed packing, whose drying rate curves are shown in Fig. 14.

Figure 14 shows drying rates obtained for some polydispersed packings. The composition of the packings is depicted in Fig. 15. The form of the curves is very similar to that of bidispersed material (compare the drying rate curve of packing a to that of the bidispersed one).

*3.2.5. Model of contact drying of bidispersed packings in a disc dryer*

In order to calculate the drying rate curves of bidispersed packings in the disc dryer we idealize the existing de-mixing, and assume a complete stratification of the two fractions. We further subdivide the drying process into two parts: (1) drying of the fine layer contacting the heating plate; (2) drying of the coarse layer lying on the fine one. These will be discussed separately. The boundary between fine and coarse product is assumed to be parallel to the heating plate, distinct and, during the drying of fine granulate, adiabatic.

(1) *Drying of the fine layer contacting the heating plate.* The drying rate of the packing during this period will be equal to the drying rate of the fine layer. The process will proceed as if no coarse material exists. The solution of Mollekopf and Schlünder can thus be applied in unchanged form.

(2) *Drying of the coarse layer.* The drying rate of the packing will now be equal to that of the coarse material. We continue to think in terms of the penetration theory and attempt to calculate the drying rate for the first static period after complete drying out of the fine product. At the beginning of this period the fine granulate will be at a temperature $T_{f,0}$ and the coarse one at $T_S$ (saturation temperature). During the static period a drying front is assumed to penetrate into the bulk of the coarse material. The situation is illustrated

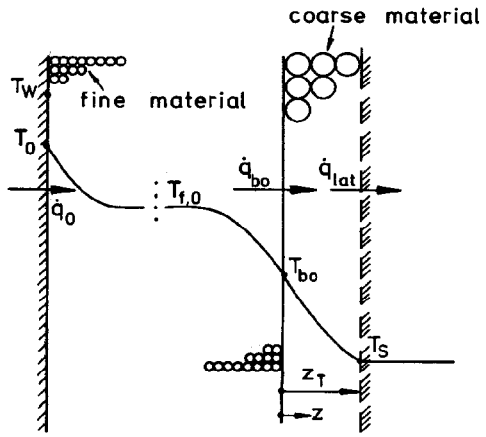


Fig. 16. The stratification model for the description of contact drying of bidispersed packings in a disc dryer. Assumed temperature profiles during the first static period after drying out of the fine-grained layer.

in Fig. 16. The general form of the temperature profiles on both sides of the layer boundary will be

$$T_f = A + B \operatorname{erf} \frac{z}{2\sqrt{\kappa_{bed,f} t}} \tag{2a}$$

$$T_c = C + D \operatorname{erf} \frac{z}{2\sqrt{\kappa_{bed,c} t}} \tag{2b}$$

Using the boundary conditions

$$z \to -\infty \Rightarrow \lim T_f = T_{f,0} \tag{3a}$$

$$z = z_T \Rightarrow T_c = T_S \tag{3b}$$

and

$$-\lambda_{bed,c} \frac{\partial T_c}{\partial z} = \rho_{bed,c} X_c \Delta h_{ev} \frac{dz}{dt} \tag{3c}$$

$$z = 0 \Rightarrow T_c = T_f \tag{3d}$$

and

$$\lambda_{bed,c} \frac{\partial T_c}{\partial z} = \lambda_{bed,f} \frac{\partial T_f}{\partial z} \tag{3e}$$

one can calculate the constants $A, B, C$ and $D$:

$$A = C = \frac{T_S + F \operatorname{erf} \zeta \, T_{f,0}}{1 + F \operatorname{erf} \zeta} \tag{4a}$$

$$B = \frac{T_S - T_{f,0}}{1 + F \operatorname{erf} \zeta} \tag{4b}$$

$$D = \frac{F(T_S - T_{f,0})}{1 + F \operatorname{erf} \zeta} \tag{4c}$$

$F$ is the ratio of the heat penetration coefficients of the two layers

$$F = \frac{\alpha^{dry}_{sb,f}}{\alpha^{dry}_{sb,c}} \tag{5}$$

with

$$\alpha^{dry}_{sb,f} = \frac{2}{\sqrt{\pi}} \frac{\sqrt{(\lambda\rho c)_{bed,f}}}{\sqrt{t_R}} \tag{6a}$$

$$\alpha^{dry}_{sb,c} = \frac{2}{\sqrt{\pi}} \frac{\sqrt{(\lambda\rho c)_{bed,c}}}{\sqrt{t_R}} \tag{6b}$$

$\zeta$ is the reduced instantaneous position of the drying front,

$$\zeta = \frac{z_T}{2\sqrt{\kappa_{bed,c} t}} \tag{7}$$

and can be calculated from

$$\sqrt{\pi}\zeta \exp(\zeta^2)(1 + F \operatorname{erf} \zeta) = \frac{c_{bed,c} F(T_{f,0} - T_S)}{X_c \Delta h_{ev}} \tag{8}$$

The time-averaged heat flux at the layer boundary as well as at the drying front can be calculated from the gradients of the temperature profile at the respective positions. It follows that

$$\dot{q}_{bo} = \left( \frac{1}{\alpha^{dry}_{sb,f}} + \frac{\operatorname{erf} \zeta}{\alpha^{dry}_{sb,c}} \right)^{-1} (T_{f,0} - T_S) \tag{9}$$

$$\dot{q}_{lat} = \dot{q}_{bo} \exp(-\zeta^2) \tag{10}$$

The average drying rate during the fictitious static period observed can be calculated from $\dot{q}_{lat}$:

$$\dot{m} = \dot{q}_{lat} / \Delta h_{ev} \tag{11}$$

The decrease in moisture content of the packing is then

$$\Delta X = \dot{m} t_R A / M_{dry} \tag{12}$$

The change in the average bulk temperature of the (dry) fine product is

$$\Delta T_f = \frac{(\dot{q}_0 - \dot{q}_{bo}) t_R A}{Q_f M_{dry} c_{bed,f}} \tag{13}$$

with $\dot{q}_0$ the time-averaged heat flux at the heating surface

$$\dot{q}_0 = \left( \frac{1}{\alpha_{ws}} + \frac{1}{\alpha^{dry}_{sb,f}} \right)^{-1} (T_W - T_{f,0}) \tag{14}$$

Assuming that, after perfect mixing, there is no heat transfer at all from dry and warm to wet and cold particles (see also ref. 4), the change in average bulk temperature of the coarse material can be calculated from

$$\Delta T_c = \frac{(\dot{q}_{bo} - \dot{q}_{lat}) t_R A}{Q_c M_{dry} (c_{bed,c} + c_L X_c)} \tag{15}$$

Equations (12), (13) and (15) provide the values of moisture content and bulk temperature at the beginning of the second static period. The entire drying rate curve can thus be calculated stepwise.

The length of the static period $t_R$ can be correlated with the time constant of the mixing device using the mixing number $N_{mix}$ (see eqn. (1)). In order to avoid renewed fitting on experimental data, we make the sweeping assumption that $N_{mix}$ has the same value for each layer as for the corresponding monodispersed packing (see Table 1). It is then

$$\alpha^{dry}_{sb,c} = \frac{2}{\sqrt{\pi}} \frac{\sqrt{(\lambda\rho c)_{bed,c}}}{\sqrt{t_{mix} N_{mix,c}}} \tag{16a}$$

$$\alpha_{sb,f}^{dry} = \frac{2}{\sqrt{\pi}} \frac{\sqrt{(\lambda\rho c)_{bed,f}}}{\sqrt{t_{mix} N_{mix,f}}} K_f \qquad (16b)$$

$K_f$ is a factor to correct the heat transfer coefficient of the fine layer for the deviation of reality from the assumed state of perfect stratification. By comparison of the calculated and measured drying rate curves the value $K_f = 2$ was found. This value was used successfully to correlate all existing measurements and appears to be not only independent of heating temperature and pressure, but, for the apparatus investigated, also of packing composition and stirrer speed.

The comparison between measurement and calculation is illustrated in Figs. 17(a)–(c) using some representative runs. The same method was used with fairly good results to predict drying rates of polydispersed packings. In order to do this, the polydispersed packing had to be divided into two parts, each of them assumed to be stochastic homogeneous (see ref. 14).

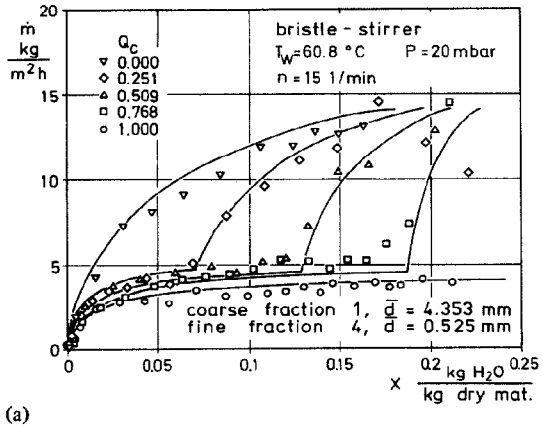


(a)

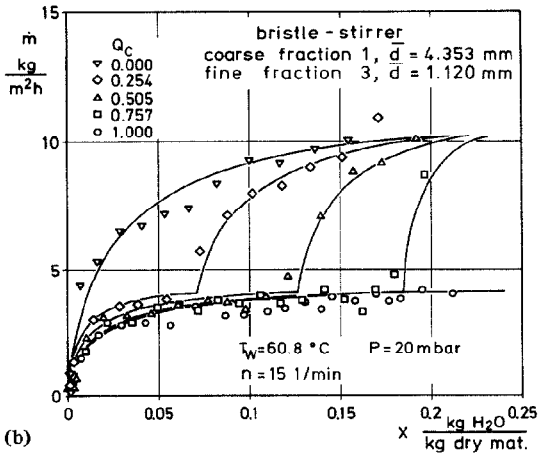


(b)

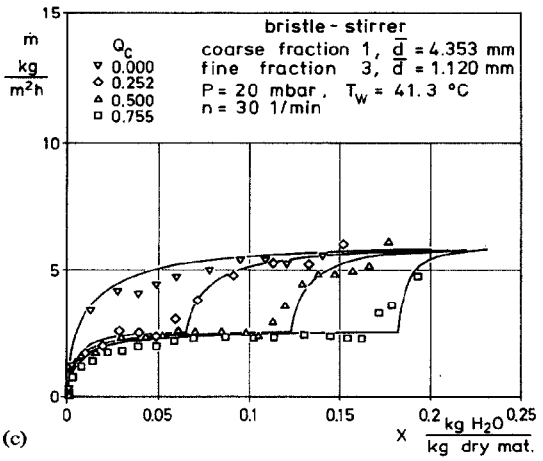


(c)

Fig. 17. Measured and calculated drying rate curves of bidispersed packings in the disc dryer.

*3.2.6. Drying of multigranular packings in the rotary drum dryer*

No measurements have been made in a drum dryer. We will, however, attempt to discuss briefly the situation likely to exist in such an apparatus, the line of attack of the problem remaining basically the same.

The de-mixing of multigranular packings in a rotary drum dryer need not and will not be the same as in the disc dryer. Possible de-mixing patterns are given by Donald and Roseman [16] (see Fig. 18). The radial de-mixing, depicted in Fig. 18 as pattern A, can be interpreted as a sort of series arrangement of monodispersed or stochastic homogeneous polydispersed regions with respect to the heating plate. It is the inverse of the case in the disc dryer, for the coarse particles are now in contact with the heating wall, thus blocking the fine granulate. The coarse granulate should thus dry first. Drying of the fine material would follow subsequently, the drying rate being radically decreased in comparison with that of monodispersed fine product. The stratification model presented in this paper would be suitable for the prediction of the drying rate.

Pattern C is an axial de-mixing, dividing the packing into monodispersed or stochastic homogeneous polydispersed bands, each of them in direct contact with the heating plate (arrangement in parallel). The drying rate can obviously be predicted as an average, weighted with the corresponding volume proportions or surface coverages, of the drying rates of fine and coarse products. Pattern B is a hybrid situation between pattern A and pattern C. It can be handled as a combination of monodispersed regions arranged partly in series and partly in parallel to each other. According to Donald and Roseman the de-mixing pattern predominating depends on the static angles of repose of the components of the mixture.

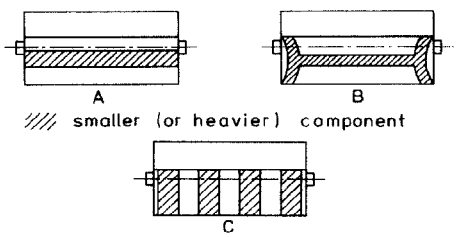


Fig. 18. De-mixing patterns in a rotating drum dryer, as reported in ref. 16.

## 4. Concluding remarks

Contact drying of granular material is commonly carried out in agitated units. If the particles of the packing differ in size or density, the mechanical agitation is likely to lead to segregation (de-mixing) of the components of the mixture, which will have a strong influence on the drying rate curve. Under certain circumstances, mixing of dry fine-grained material in a bed of coarse-grained product can improve the drying rate of the latter.

The model introduced by Mollekopf and Schlünder to predict the drying rate during vacuum contact drying of free flowing mechanically agitated particulate material can be extended in order to describe such cases.

## Acknowledgement

The authors thank the AIF (Arbeitsgemeinschaft Industrieller Forschungsvereinigungen) and the Forschungsvereinigung für Luft- und Trocknungstechnik, Frankfurt-on-Main, for the financial support of this work.

## Nomenclature

| | |
|---|---|
| $A$ | hot surface area, $m^2$ |
| $A, B, C, D$ | constants, eqns. (2a), (2b) |
| $c$ | specific heat, $J\,kg^{-1}\,K^{-1}$ |
| $d$ | particle diameter, m |
| $D$ | dryer diameter, m |
| $F$ | ratio of heat penetration coefficients, eqn. (5) |
| $\Delta h_{ev}$ | latent heat of evaporation, $J\,kg^{-1}$ |
| $K_f$ | correction coefficient, eqn. (16b) |
| $\dot{m}$ | drying rate, $kg\,m^{-2}\,s^{-1}$ |
| $M$ | mass, kg |
| $n$ | number of revolutions of mixing device, $s^{-1}$ |
| $N_{mix}$ | mixing number, eqn. (1) |
| $P$ | pressure, mbar |
| $\dot{q}$ | heat flux, $W\,m^{-2}$ |
| $Q$ | mass of component to total mass of packing (dry) |
| $R$ | particle radius, m |
| $t$ | time, s |
| $T$ | temperature, K |
| $X$ | moisture content, (kg moisture)/(kg dry material) |
| $z$ | length normal to hot surface, m |
| $z_T$ | penetration depth, m |
| $\alpha$ | heat transfer coefficient, $W\,m^{-2}\,K^{-1}$ |
| $\beta$ | mass transfer coefficient, $m\,s^{-1}$ |
| $\delta$ | surface roughness, m |
| $\zeta$ | reduced penetration depth |
| $\kappa$ | thermal diffusivity, $m^2\,s^{-1}$ |
| $\lambda$ | thermal conductivity, $W\,m^{-1}\,K^{-1}$ |
| $\rho$ | density, $kg\,m^{-3}$ |
| $\psi$ | porosity |

*Indices*

| | |
|---|---|
| b | bulk |
| bed | bed |
| bo | at boundary |
| c | coarse-grained product |
| dry | dry |
| f | fine-grained product |
| lat | latent |
| loc | local |
| L | liquid |
| mix | mixing |
| P | particle |
| R | static period |
| S | saturation |
| sb | bulk |
| T | at drying front |
| W | wall |
| ws | wall-to-bed |
| 0 | at beginning |
| 0 | at hot surface |

## References

1 S. Günes, Kontakttrocknung von grobkörnigen mechanisch durchmischten Schüttungen im Vakuum, *Dissertation*, Karlsruhe, 1979.
2 R. M. Carn and J. C. King, Modification of conventional freeze-dryers to accomplish limited freeze-drying, *AIChE Symp. Ser.*, (163) (1973) 103–112.
3 H. G. Kessler, Gefriertrocknung mit Produktumlagerung, *Vt-Verfahrenstechnik, 8* (1974) 348–355.
4 N. Mollekopf, Wärmeübertragung an mechanisch durchmischtes Schüttgut mit Wärmesenken in Kontaktapparaten, *Dissertation*, Karlsruhe, 1983.
5 E. U. Schlünder and N. Mollekopf, Vacuum contact drying of free flowing mechanically agitated particulate material, *Chem. Eng. Process., 18* (1984) 93–11.
6 E. U. Schlünder, Wärmeübergang an bewegte Kugelschüttungen bei kurzfristigem Kontakt, *Chem.-Ing.-Tech., 43* (1971) 651–654.
7 R. Bauer, in *VDI-Wärmeatlas*, VDI-Verlag, Düsseldorf, 4th edn., 1984.
8 E. U. Schlünder, Heat transfer to packed and stirred beds from the surface of immersed bodies, *Chem. Eng. Process., 18* (1984) 31–53.
9 E. Tsotsas and E. U. Schlünder, Contact drying of mechanically agitated particulate material in the presence of inert gas, *Chem. Eng. Process., 20* (1986) 277–285.
10 R. Bauer and E. U. Schlünder, Effective radial thermal conductivity of packings in gas flow, Part II. Thermal conductivity of the packing fraction without gas flow, *Int. Chem. Eng., 18* (1978) 181–203.
11 M. E. Wise, Dense random packing of unequal spheres, *Philips Res. Rep., 7* (1952) 321–343.
12 J. A. Dodds, The porosity and contact points in multicomponent random sphere packings calculated by a simple statistical geometric model, *J. Colloid Interface Sci., 77* (1980) 317–327.
13 R. Jeschar, Druckverlust in Mehrkornschüttungen aus Kugeln, *Arch. Eisenhüttenwes., 35* (1964) 91–108.
14 E. Tsotsas, Über den Einfluss der Dispersität und der Hygroskopizität auf den Trocknungsverlauf bei der Vakuum-Kontakttrocknung rieselfähiger Trocknungsgüter, *Dissertation*, Karlsruhe, 1985.
15 J. Wunschmann, Wärmeübergang von beheizten Flächen an bewegte Kugelschüttungen bei Normaldruck und im Vakuum, *Dissertation*, Karlsruhe, 1985.
16 M. B. Donald and B. Roseman, Mechanisms of mixing in a horizontal drum mixer, *Br. Chem. Eng., 7* (1962) 749–753.